

PAPER • OPEN ACCESS

Raster image processing using 2D Padé-type approximations

To cite this article: V I Olevskiy *et al* 2023 *J. Phys.: Conf. Ser.* **2675** 012015

View the [article online](#) for updates and enhancements.

You may also like

- [Zero distribution for Angelesco Hermite–Padé polynomials](#)
E. A. Rakhmanov
- [In vivo magnetic resonance spectroscopy by the fast Padé transform](#)
Dževad Belki and Karen Belki
- [Exact quantification of time signals in Padé-based magnetic resonance spectroscopy](#)
Dževad Belki

PRIME
PACIFIC RIM MEETING
ON ELECTROCHEMICAL
AND SOLID STATE SCIENCE

HONOLULU, HI
Oct 6–11, 2024

Abstract submission deadline:
April 12, 2024

Learn more and submit!

Joint Meeting of
The Electrochemical Society
•
The Electrochemical Society of Japan
•
Korea Electrochemical Society

Raster image processing using 2D Padé-type approximations

V I Olevskiy¹, Yu B Olevska², O V Olevskiy³ and V V Hnatushenko¹

¹ Department of Information Technology and Computer Engineering, Dnipro University of Technology, 19 Dmytro Yavornytskyi Avenue, Dnipro, 49005, Ukraine

² Department of Applied Mathematics, Dnipro University of Technology, 19 Dmytro Yavornytskyi Avenue, Dnipro, 49005, Ukraine

³ Department of Computer Technologies, Oles Honchar Dnipro National University, 72 Gagarina Avenue, Dnipro, 49010, Ukraine

Olevskiy.V.I@nmu.one

Abstract. We have developed a method called the two-dimensional Padé-type approximants method, which can be used to reduce the Gibbs phenomenon in the harmonic two-dimensional Fourier series. This method can be applied to both monochrome and color raster images. To do this, we implement the generalized two-dimensional Padé approximation proposed by Chisholm. In this approach, we select the range of frequency values on the integer grid according to the Vavilov method. We propose a definition of a Padé-type functional and provide examples of its application to simple discontinuous templates represented as raster images. Through this study, we are able to draw conclusions about the practical usage and advantages of the Padé-type approximation. We demonstrate that the Padé-type approximant effectively eliminates distortions associated with the Gibbs phenomenon, and it is visually more appropriate than the Fourier approximant. Additionally, the application of the Padé-type approximation reduces the number of parameters without sacrificing precision.

1. Introduction

The primary method of displaying graphic files on a computer screen is through raster images. These images are created by compiling pixels, each containing unique color and tonal information, to form the overall image. Raster image files consist of a rectangular array of pixel parameter values, typically stored in a compressed format. Depending on the type of compression used, it may or may not be possible to fully restore the original image.

Expanding a raster image signal into a two-dimensional Fourier series is a common approach to reducing the size of the graphic file. However, this often results in significant distortions, particularly due to the Gibbs effect. The Gibbs phenomenon is a property of one-dimensional Fourier series that occurs when a discontinuous periodic function is truncated, and only a finite number of terms are used [1-3]. This truncation causes distortions near the points of discontinuity, which cannot be eliminated by increasing the number of series terms.

In the case of two-dimensional images, the Gibbs phenomenon significantly degrades the quality of processed images for most popular graphic standards that utilize a finite sum of harmonics. Distortions occur along the borders of sharp contrast changes, resulting in the appearance of false optical shadows. This negative impact on image quality also affects the analysis of x-ray and sonar studies when processing their results.



The presence of the Gibbs phenomenon is not limited to one-dimensional signals but also applies to the two-dimensional case. This phenomenon has a significant negative impact on the quality of image processing in widely-used graphic standards that rely on a finite sum of harmonics [2]. Distortions occur along the borders where there are sharp changes in contrast, resulting in the false appearance of optical shadows [3, 4]. This issue is particularly problematic when analyzing the results of x-ray and sonar studies. In the context of magnetic resonance imaging (MRI), the Gibbs phenomenon manifests as a type of artifact. In MRI images, parallel lines can be observed that are associated with abrupt and intense changes in the object being imaged, such as the CSF-spinal cord and skull-brain interface [4, 5].

The field of mathematical physics approximation is experiencing rapid development, with the theory of approximation being the most prominent area of progress [1, 6, 7]. Traditionally, the focus has been on approximation techniques that utilize polynomials [8, 9] and trigonometric functions [6, 7, 10]. One particularly successful type of approximation technique is the use of fractional rational functions [8, 11, 12]. The interest in this type of approximation has been steadily growing due to its wide range of applications in various fields, including theoretical physics, applied mechanics, geophysics, and more [8, 11, 12]. These techniques enable the generalized summation of series and the extension of the function being approximated into the meromorphic domain.

Lately, there has been a significant focus on extending the classical theory of approximation using fractional-rational functions. This includes exploring different types of basis functions and various methods of constructing approximants, such as Padé-type approximations [12, 14-19]. By carefully selecting the construction method, significant enhancements in the desirable properties of the approximants can be achieved for specific classes of functions [12-14].

The objective of this study is to address two main goals: eliminating the Gibbs phenomenon in image processing and reducing the size of resulting image files. To accomplish this, we propose utilizing the two-dimensional Padé-type approximants method that we have previously developed. This method has shown promise in achieving these objectives in our previous work [12].

2. Technic of Padé-type approximants usage

2.1. Connection establishing between power series and Fourier series for construction of Padé-type approximants

In our approach, we aim to construct Padé-type approximants for the harmonic two-dimensional Fourier series as a subset of power series [12]. In order to achieve this, we will present some basic principles of construction. We consider the separable space $L_2[(a_2, b_2) \times (a_2, b_2)]$ of two-dimensional complex functions $f(x_1, x_2)$, which are integrable on this finite or infinite rectangle. We can choose a countable set of functions

$$B_i = \{e_{ij}, j = \overline{1, \infty}, i = \overline{1, 2}, \quad (1)$$

as a basis of space with respect to individual coordinates.

In the situation involving trigonometric functions, the fundamental functions can be expressed in the following manner:

$$e_{nk} = e^{ikx_n} = (e^{ix_n})^k = (e_{n1})^k, n = 1, 2. \quad (2)$$

In the given context, the representation of an arbitrary function in the considered space based on the given basis as in equation (2) can be viewed as a two-dimensional generalized power series in the following form:

$$f = \sum_{k,p=1}^{\infty} a_{kp} (e_{11})^k (e_{21})^p. \quad (3)$$

In [12] we have proposed the definition of the functional of the Padé-type in following form.

Definition. Suppose a two-dimensional power series $S = \sum_{k,p=1}^{\infty} a_{kp} (x_1)^k (x_2)^p$ of complex variables x_1, x_2 and the associated Padé approximant $P[m_1, n_1 / m_2, n_2](x_1, x_2)$ in the proper sense are given. Then the Padé-type functional $GP = \sum_{k,p=1}^{\infty} a_{kp} (x_1)^k (x_2)^p$ associated with the given generalized power series $GS = \sum_{k,p=1}^{\infty} a_{kp} (f_1)^k (f_2)^p$ for the complex functions of these variables is defined as

$$GP_{GS}[m_1, n_1 / m_2, n_2](f_1, f_2) = P[m_1, n_1 / m_2, n_2](x_1, x_2) \Big|_{x_1=f_1, x_2=f_2} \cdot \quad (4)$$

The construction process of Padé approximant is outlined as follows:

1. We first select the types of bases for the individual variables as in equation (1).
2. The function f that we want to approximate is then represented in the form as in equation (3).
3. We construct a Padé approximant $P[m_1, n_1 / m_2, n_2](x_1, x_2)$ in the proper sense for the power series of two complex variables x_1, x_2 using coefficients which correspond to the representation as in equation (3).
4. Finally, we apply a substitution of the basis functions into a functional of Padé-type as shown in equation (4).

The suggested method enables the determination of the essential and complete set of coefficients for constructing a Padé-type approximant with a predefined numerator and denominator structure.

2.2. Technic of Padé-type approximants construction

Suppose we have a function $f(x_1, x_2)$ of monochrome image point brightness in the range of $[0, 1]$ on the rectangle $(a_2, b_2) \times (a_2, b_2)$. It can be approximately represented in form of truncated Fourier series

$$f(x_1, x_2) \approx \sum_{m=0}^M \sum_{n=0}^N f_{mn} \cos(m\lambda_1 x_1) \cos(n\lambda_2 x_2).$$

Let's denote it's Padé approximant $P[m_1, n_1 / m_2, n_2](x_1, x_2)$ as $P(x_1, x_2)$. Then to obtain cosine part of two-dimensional exponent, we use the following equality [18]:

$$f(x_1, x_2) \approx \frac{1}{2} \operatorname{Re} [P(x_1, x_2) + P(x_1, -x_2)]. \quad (5)$$

In cases where the image is stored as a two-dimensional array of points, such as a bmp file, the Padé approximation can be implemented using discrete Fourier transform (DFT) procedures [2]. DFT serves as the foundation for various image and video compression algorithms, including the widely used jpeg and mpeg standards for compressing both still and video images.

To perform the Padé approximation, the input image is first decomposed into spectral components using a two-dimensional discrete cosine transform (2D DCT). The 2D DCT can be computed by applying a one-dimensional DCT algorithm to each row or column of the two-dimensional matrix representing the input signal. This is possible because the DCT is a separable function. The direct calculation of the 2D DCT for an $M \times N$ matrix of a two-dimensional signal $f(x, y)$ can be expressed as:

$$F(u, v) = \frac{2}{\sqrt{MN}} C(u) C(v) \sum_{n=0}^{N-1} \sum_{m=0}^{M-1} f(n, m) \cos\left(\frac{\pi(2n+1)u}{2N}\right) \cos\left(\frac{\pi(2m+1)v}{2M}\right) \quad (6)$$

where $C(x) = 2^{-0.5}$ for $x = 0$ and $C(x) = 1$ for $x \neq 0$.

Coefficients of a truncated cosine Fourier series for $f(x_1, x_2)$ can be obtained as the values of $F(u, v)$ in equation (6), divided by the step.

Afterwards, the Vavilov method is employed to select the range of frequency values on the integer grid [13]. The size of this range directly influences the number of equations that need to be generated.

To achieve this objective, we employ Chisholm's suggested method for the generalized two-dimensional Padé approximation when $N=M$ [11]. In the case where $f(x, y)$ represents a function of two variables, it can be represented as a power series in two dimensions of the form

$$f(x, y) = \sum_{k,p=1}^{\infty} a_{kp} x^k y^p$$

expressing the N -th Chisholm approximation can be done as follows:

$$f_{N,N}(x, y) = \left(\sum_{k,p=1}^N p_{kp} x^k y^p \right) \left(\sum_{k,p=1}^N q_{kp} x^k y^p \right)^{-1}$$

If we utilize a collection of power values that is confined within a right triangle where the legs correspond to the axes, then we can determine the coefficients p_{kp} and q_{kp} by employing the subsequent equations:

$$\sum_{\sigma=0}^{\gamma} \sum_{r=0}^{\delta} q_{\sigma r} a_{\gamma-\sigma, \delta-r} = p_{\gamma\delta}, (\gamma, \delta = 0, 1, \dots, 2N, 1 \leq \delta + \gamma \leq 2N), \tag{7}$$

$$\sum_{\sigma=0}^{\gamma} \sum_{r=0}^{\delta} (q_{\sigma r} a_{\gamma-\sigma, \delta-r} + q_{r\sigma} a_{\delta-r, \gamma-\sigma}) = 0, (\gamma = 1, 2, \dots, 2N, \delta + \gamma = 2N), p_{00} = 1.$$

The solution of this system of equations is a matrix of coefficients p and q .

In our investigations we use the Vavilov method for obtaining approximants coefficients [12]. In this case we use only equation (7) but for a set of power values bounded by two rectangles as it shown in figure 1 and supposing $p_{\gamma\delta} = 0, (\gamma, \delta > N)$.

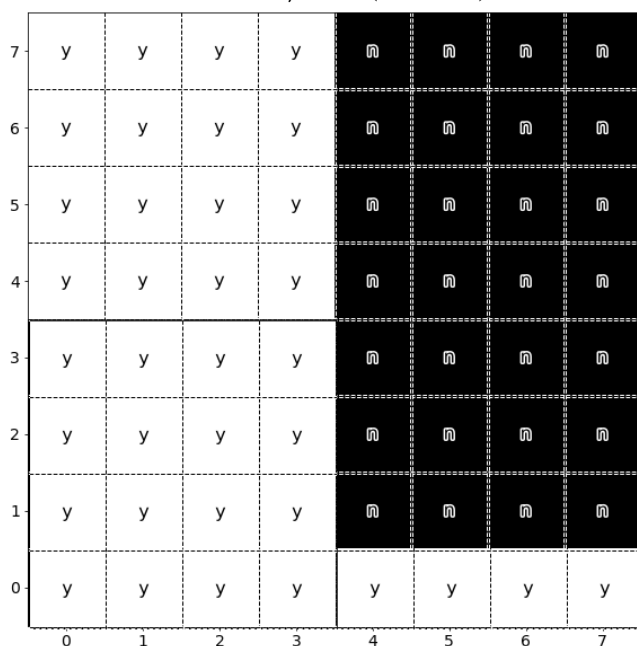


Figure 1. An integer grid of power values for the Vavilov method when $N=4$: white points with “y” are used for calculations, and black points with “n” aren’t.

The process of compressing two-dimensional signals using two-dimensional discrete cosine transformation description can be found in reference [12].

3. Examples of Padé-type approximants application

3.1. Examples for monochrome image case

Here we examine the utilization of Padé-type approximations to basic, non-continuous template functions in both symbolic and discrete forms [12].

3.1.1. Example for formulaic representation of raster. In the general case, such a representation of a raster image assumes the presence of Fourier series already calculated analytically for the brightness function [2].

Let's examine a template function in a periodic form with a period of 2π

$$f(x_1, x_2) = \begin{cases} 1, & x_1^2 + x_2^2 \leq \pi, \\ 0, & x_1^2 + x_2^2 > \pi. \end{cases}$$

This function is symmetrical about both x_1 and x_2 axes. Therefore, the truncated Fourier series is considered to be the most appropriate method for its approximation in form

$$f(x_1, x_2) \approx \sum_{m=0}^4 \sum_{n=0}^4 f_{mn} \cos(mx_1) \cos(nx_2)$$

We utilized the Padé-type approximation with a structure of $[2,2 / 2,2]$ to equation (6), taking a subset of previously derived Fourier coefficients without any supplementary information. To extract the cosine component of the two-dimensional exponent, we applied the inverse transformation as in equation (5) to the Padé-type approximant. The initial raster image, the desired real approximation and image Fourier series representation is shown in column No 1 in table 1.

Table 1. Initial and restored monochrome images.

No	1	2	3	4	5	6	7
Raster image							
Padé-type approximant							
Fourier series with compression							
Number of harmonics for minimum error	8	7	6	4	4	5	8

The transformation used for the cosine series in this context is identical to the one employed in the field of radio physics [10].

The image shows distortions that are inherent to the Gibbs phenomenon in the Fourier series, but these distortions are effectively absent in the Padé-type approximant. It is clear that the Padé-type approximant is visually more appropriate than the Fourier series.

In order to assess the accuracy of both the Fourier series method and the Padé-type approximation, we have included a comparison of their respective one-dimensional sections with the template function in figure 2. This comparison highlights the advantage of using the Padé approximation.

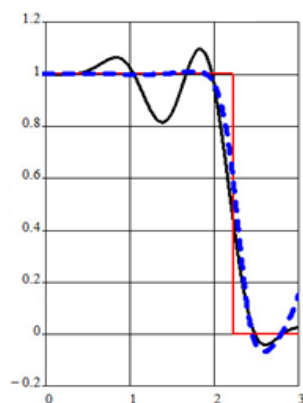


Figure 2. The profiles of the approximations and the template function along line $x_1 = x_2$: red – the template, black – Fourier series, dashed blue – Padé-type approximant.

3.1.2. Examples for discrete representation of raster. In our study, we selected six monochrome symmetrical bitmap test images from the digital library [20], which are listed in columns No 2-7 of table 1. For asymmetrical input signals, we artificially expanded the images to make them symmetrical.

To reduce the file size according to the jpeg standard, insignificant decomposition coefficients were excluded. We applied this method by processing the results of 2D DCP on the input images, considering the rapid decline of harmonic amplitudes. The resulting image was used for comparison with the quality of the image compressed by the proposed method. The standardized root mean square error and the normalized mean absolute error were used as criteria for comparison. The size of the area on the integer grid ranged between 2 and 8, and the number of coefficients used for reconstructing the compressed image was gradually increased. For the compressed image, this number (and thus the file size) was approximately half of the original value.

3.2. Example for color image case

Let's consider processing of color images in RGB format [2]. The main objective of the RGB color model is to facilitate the sensing, representation, and display of images in electronic systems like computers and televisions. This model employs the additive color approach, where the primary colors of red, green, and blue light are combined with varying intensities to reproduce a wide range of colors in a pixel. So, instead one matrix of brightness of monochrome image point, we have three matrixes coinciding every color. and proposed technic can be used for processing every color matrix separately.

The jpeg format, which is most used for storing bitmap files, divides the original image into blocks of 8x8 pixels, followed by processing each block using DCT separately (figure 3).

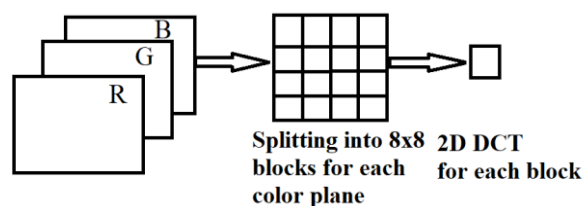


Figure 3. Part of an algorithm for processing of 2D color raster images in jpeg format.

The proposed technic was used for color bitmap "Test card Philips PM5544" (GNU Free Documentation License) [21]. Consecutive image processing steps are presented in figure 4.

4-th Chisholm approximation is used for each 8x8 block of every color matrix. Results of comparison are represented in figure 5. In the approximate calculation of the parameters of the Padé-type approximation, the appearance of conjugate false poles and zeros is possible [11, 22]. This can lead to image scaling failure. It should be noted that similar scaling violations also occur when deploying jpeg files [23]. This phenomenon is eliminated either by cutting off the values of the brightness function, or by using an averaging filter. For this purpose, other methods developed by us for increasing the spatial

resolution of multispectral images with automation of the choice of the best pansharpening method can be effectively applied [24, 25].

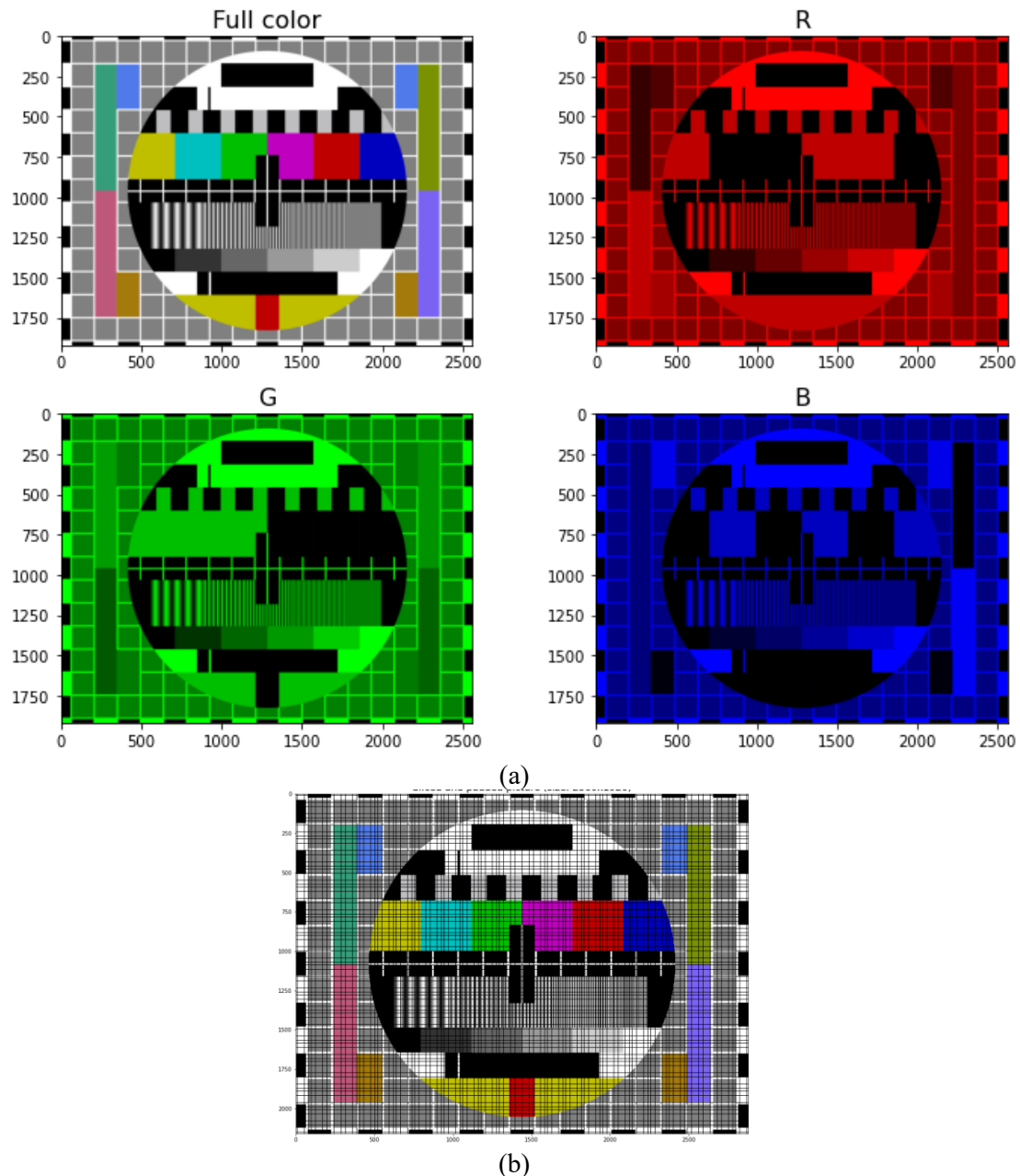


Figure 4. The algorithm steps for processing of 2D color raster images: (a) – color division, (b) – 8x8 blocks division.

The results shown in figure 5 illustrate that the suggested approach successfully approximates the original image in terms of both clarity and color reproduction. Although there are minor clarity distortions found only in areas with very high spatial frequencies, they do not significantly impact the overall perception of the image. Therefore, the proposed method is suitable for storing and displaying color raster images on electronic devices effectively.

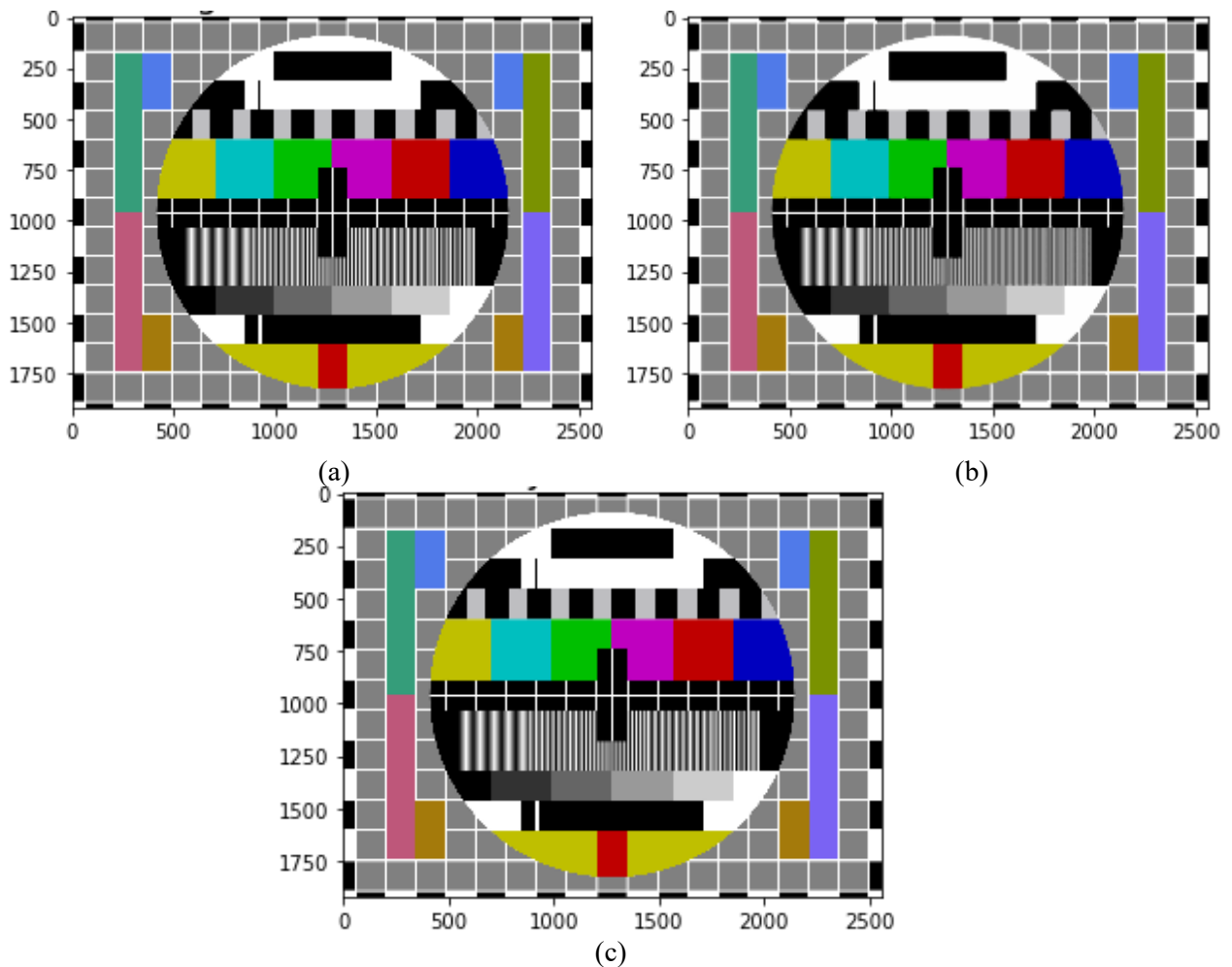


Figure 5. Comparison of processing results: (a) – original raster image, (b) – proposed technics result, (c) – jpeg format image.

4. Analysis of Padé-type approximants usage

Upon studying the mean square error graphs of the images enumerated in table 1, it is noticeable that as the visual similarity between the image and the original improves, there is a substantial reduction in the mean square error. The findings obtained from evaluating the criteria demonstrate that each image type possesses its own distinct threshold, at which point the reconstructed image achieves visual resemblance to the original (see table 1).

The analysis of the Padé-type approximation method and its benefits allows us to draw certain conclusions.

Firstly, Figure 6b illustrates that the Padé approximation exhibits a lower level of noise compared to the Fourier series for the cosine (Figure 6a).

Secondly, the utilization of the Padé-type approximation considerably reduces the number of approximant parameters without compromising accuracy (and sometimes even improving it). Specifically, the Fourier series with N harmonics in both directions requires N^2 parameters. However, employing the Padé-type approximation with the numerator and denominator powers equal to $N/2$ results in $N^2/2 - 1$ parameters, reducing the number of parameters by more than half.

The results obtained demonstrate that the Padé-type approximant effectively eliminates the distortions inherent to the Gibbs phenomenon. It is clear that the Padé-type approximant is visually more appropriate than the Fourier series for both monochrome and color images.

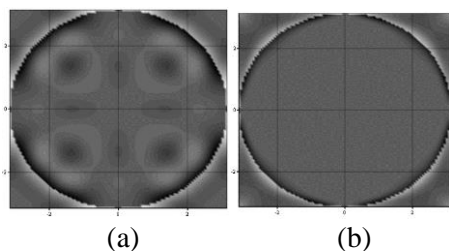


Figure 6. The discrepancies between the template functions and their corresponding approximations for (a) – Fourier cosine series, (b) – Padé approximation

Additionally, using the Padé-type approximation reduces the number of parameters without sacrificing precision. The software that implements this method is suitable for practical use and, furthermore, it can serve as a theoretical basis for developing a new effective color image format in addition to the jpeg format [2, 12].

Acknowledgments

The work is supported by the state budget scientific research project of Dnipro University of Technology “Models and information technologies of data processing and analysis in complex computer systems and networks” (state registration number 0121U114523).

References

- [1] Olevskiy V and Olevska Y 2018 Geometric aspects of multiple Fourier series convergence on the system of correctly counted sets *Geom. Integr. Quantization* **19** 159–167
- [2] Mitra S K 2010 *Digital Signal Processing: A Computer-Based Approach* (New York: McGraw-Hill)
- [3] Helmberg G 2002 Localization of a Corner-Point Gibbs Phenomenon for Fourier Series in Two Dimensions *J. Fourier Anal. Appl.* **8** 29–42
- [4] Archibald R and Gelb R 2002 A method to reduce the Gibbs ringing artifact in MRI scans while keeping tissue boundary integrity *IEEE Trans. Med. Imaging* **21** 305–319
- [5] Veraart J, Fieremans E, Jelescu I O, Knoll F and Novikov D S 2016 Gibbs ringing in diffusion MRI *Magn. Reson. Med.* **76** 301–314
- [6] Olevskiy V and Olevska Y 2018 Mathematical model of elastic closed flexible shells with nonlocal shape deviations *J. Geom. Symmetry Phys.* **50** 57–69
- [7] Maggioli F, Melzi S, Ovsjanikov M, Bronstein M M and Rodolà E 2021 Orthogonalized fourier polynomials for signal approximation and transfer *Comput. Graph. Forum* **40** 435–447
- [8] Andrianov I, Olevskiy V I and Olevska Y B 2017 *AIP Conf. Proc.* **1895** 080001 <https://pubs.aip.org/aip/acp/article-abstract/1895/1/080001/696845/Asymptotic-estimation-of-free-vibrations-of?redirectedFrom=fulltext>
- [9] Mossakovskii V I, Mil'tsyn A M, Selivanov Yu M and Olevskii V I 1994 Automating the analysis of results of a holographic experiment *Strength Mater.* **26**(5) 385–391
- [10] Drobakhin O O, Olevskiy O V and Olevskiy V I 2017 *AIP Conf. Proc.* **1895** 060001 <https://pubs.aip.org/aip/acp/article-abstract/1895/1/060001/696883/Study-of-eigenfrequencies-with-the-help-of-Prony-s?redirectedFrom=fulltext>
- [11] Baker J A Jr and Graves-Morris P 1996 *Padé approximants* (New York: Cambridge University Press)
- [12] Olevskiy V I, Hnatushenko V V, Korotenko G M, Olevska Yu B and Obydennyi Y O 2023 Application of two-dimensional Padé-type approximations for image processing *Radio Electronics, Computer Science, Control* **1** 99-106
- [13] Olevskiy V I, Smetanin V T and Olevska Yu B 2017 *AIP Conf. Proc.* **1895** 070003 <https://pubs.aip.org/aip/acp/article-abstract/1895/1/070003/696753/Fuzzy-method-of-recognition-of-high-molecular?redirectedFrom=fulltext>
- [14] Labych Yu A and Starovoitov A P 2009 Trigonometric Padé approximants for functions with regularly decreasing Fourier coefficients *Sb. Math.* **200** 1051–1074

- [15] Buslaev V I and Suetin S P 2016 On the existence of compacta of minimal capacity in the theory of rational approximation of multi-valued analytic functions *J. Approx. Theory.* **206** 48–67
- [16] Holub A P and Lysenko L O 2017 Padé approximants for some classes of multivariate functions *Ukrains'kyi Matematychnyi Zhurnal* **69** 631–40
- [17] Holub A P 2014 Many-dimensional generalized moment representations and Padé-type approximants for functions of many variables *Ukrains'kyi Matematychnyi Zhurnal* **66** 1166–1174
- [18] Bosuwan N and López Lagomasino G 2015 Inverse theorem on row sequences of linear Padé-orthogonal approximation *Comput. Methods Funct. Theory* **15** 529–554
- [19] Daras, N.J. 2003 Generalized Padé-type approximation and integral representations *Adv. Comput. Math.* **18** 1–39
- [20] TESTIMAGES free collection of digital images for testing *Access mode:* <https://testimages.org/Received 00.00.2023>.
- [21] Ebnz 2008, Jun. 13 Test card Philips PM5544 *Access mode:* https://en.wikipedia.org/wiki/File:Philips_PM5544.svg
- [22] Yamada H and Ikeda K 2014 A Numerical Test of Padé approximation for some functions with singularity *International Journal of Computational Mathematics* **2014**
- [23] Khalid Y Understanding and Decoding a JPEG Image using Python *Access mode:* <https://yasoob.me/posts/understanding-and-writing-jpeg-decoder-in-python/>
- [24] Hnatushenko V and Kashtan V 2021 Automated pansharpening information technology of satellite images *Radio Electronics, Computer Science, Control* **2** 123–132
- [25] Gnatushenko V 2003 The use of geometrical methods in multispectral image processing *J. Autom. Inf. Sci.* **35** 1–8